

## Article

# Design of Highly Efficient Nickel-Cobalt-Manganese-Molybdenum (NCMM) Nano-Catalysts Supported on Activated Carbon for Desulfurization Process

Shymaa A. Hameed <sup>1,2</sup>, Raja Ben Amar <sup>3</sup>, Khaleel I. Hamad <sup>4</sup> , Aysar T. Jarullah <sup>2</sup> and Iqbal M. Mujtaba <sup>5,\*</sup> <sup>1</sup> National Engineering School of Gabes, Gabes University, Gabes 6029, Tunisia; sh.a.hamed@tu.edu.iq<sup>2</sup> Chemical Engineering Department, College of Engineering, Tikrit University, Tikrit P.O. Box 42, Iraq; a.t.jarullah@tu.edu.iq<sup>3</sup> Faculty of Science of Sfax, University of Sfax, Sfax 3038, Tunisia; raja.rekik@fss.rnu.tn<sup>4</sup> The Open Educational College, Salah El-Din Study Center, Ministry of Education, Tikrit P.O. Box 55, Iraq; khalil.edan@tu.edu.iq<sup>5</sup> Department of Chemical Engineering, Faculty of Engineering & Informatics, University of Bradford, Bradford BD7 1DP, UK

\* Correspondence: i.m.mujtaba@bradford.ac.uk

**Abstract:** To maintain a healthy environment and way of life in the modern world, clean fuel must be produced. It is important to totally and successfully remove sulfur-containing harmful compounds from fuel oil in order to comply with the new sulfur legislation. Numerous methods have been proposed in the literature for desulfurizing fuel oil. In this study, activated carbon (AC), which is regarded as a significant porous material, is derived from agro-wastes such as apricot shells (AS) and is loaded with different combinations of active metals. Nickel–Cobalt–Manganese (NCM) over AC is firstly prepared and evaluated experimentally. Then, several concentrations of Molybdenum (1%, 2% and 3%) are separately added to NCM to generate three novel composite mesoporous nano-catalysts (NCMM\_1, NCMM\_2 and NCMM\_3). Several tests have been carried out to determine the catalysts' properties, such as BET<sub>surface area</sub>, pore volume, FTIR, TGA and SEM, XRF and XRD. These catalysts are then used in the batch oxidative desulfurization process to remove sulfur compounds from wide cut oil (from IBP to 345 °C). The pilot plant conditions were as follows: air flow rate = 120 L/h, reaction temperature = 363 K and reaction time of 1 h for all catalysts. Remarkable characteristics have been noticed, and it was discovered that the nano-catalyst NCMM\_2 performed better in terms of degree of sulfur removal compared to other nano-catalysts.

**Keywords:** nano-catalyst; ODS; apricot shell; activated carbon; wide middle distillate

**Citation:** Hameed, S.A.; Amar, R.B.; Hamad, K.I.; Jarullah, A.T.; Mujtaba, I.M. Design of Highly Efficient Nickel-Cobalt-Manganese-Molybdenum (NCMM) Nano-Catalysts Supported on Activated Carbon for Desulfurization Process. *Catalysts* **2023**, *13*, 1196. <https://doi.org/10.3390/catal13081196>

Academic Editors: Salette Balula and Fátima Mirante

Received: 6 July 2023

Revised: 31 July 2023

Accepted: 5 August 2023

Published: 10 August 2023



**Copyright:** © 2023 by the authors. Licensee MDPI, Basel, Switzerland. This article is an open access article distributed under the terms and conditions of the Creative Commons Attribution (CC BY) license (<https://creativecommons.org/licenses/by/4.0/>).

## 1. Introduction

Enhancing catalysts for catalytic activity is a crucial issue for reducing toxic contaminants in industrial processes, such as petroleum refineries. The choices of catalyst type, manufacturing process and materials significantly impact environmentally friendly fuel production. When petroleum or oil fractions and natural gas are burned, harmful gases are released into the atmosphere, which has adverse effects on both the environment and human health. Therefore, sulfur and the hard compounds (mainly heavy metals, nitrogen and asphaltene) can be highly reactive, leading to poison catalysts being used and damaging refining machinery. The European Union (EU) and the United States (US) have implemented rules limiting the release of sulfur between 10 and 15 ppm in order to minimize pollution in the atmosphere and technological problems [1,2]. In petroleum products, there are substances containing organic sulfur compounds, such as thiol, thiophene (TH), benzothiophene (BT), dibenzothiophene (DBT) and others, in nature [3,4]. The current technique for lowering the sulfur level of petroleum is hydrodesulfurization (HDS). High pressure and temperature are presented during this process; as well, high

hydrogen consumption is found [5,6]. However, because of the insufficient treatment of benzothiophene and dibenzothiophene, it is unable to achieve ultra-low sulfur criteria [7]. Therefore, it is essential that refineries are looking for new methods to create ultra-low sulfur fuel. Over the past few years, alternative technologies have been researched, and among them, oxidative treatments, specifically the oxidative desulfurization (ODS) process, can be highlighted. In addition, the research and choice of catalysts are critical in ODS, as they are in any catalytic process. Under mild conditions, oxidative desulfurization (ODS) can be especially efficient and considered a possible method for eliminating the BT, DBT and other derivatives of sulfur compounds from petroleum products.

The catalytic ODS technique is a type of technology that uses oxidants to oxidize the organic sulfur in two stages: the first process involves oxidizing the sulfur molecules into strong polarity molecules, and the second step involves a separation process, such as extraction using a solvent, to efficiently separate these polar products. Using a variety of oxidizing agents, including  $\text{HNO}_3$ ,  $\text{NO}_2$ ,  $\text{H}_2\text{O}_2$ ,  $\text{NaBrO}_3$ , TBHP, air, ozone, etc., in the presence of a catalyst, ODS converts sulfur-containing fuel molecules into sulfoxides and sulfone compounds, alternately [8–10]. Regarding the development of research on ODS catalysts, it is becoming clear that catalytic structuring is important for obtaining selective oxidation of sulfur compounds. In general, catalysts typically encourage the production of reactive oxygen types using the most desired oxidants, including oxygen and hydrogen peroxide and, as a result, speed up the ODS process [11]. Based on the literature, it is found that a variety of catalysts from simple acids to solid composite materials are used in ODS. Figure 1 shows a pathway for the removal of sulfur by an oxidation reaction [12,13].

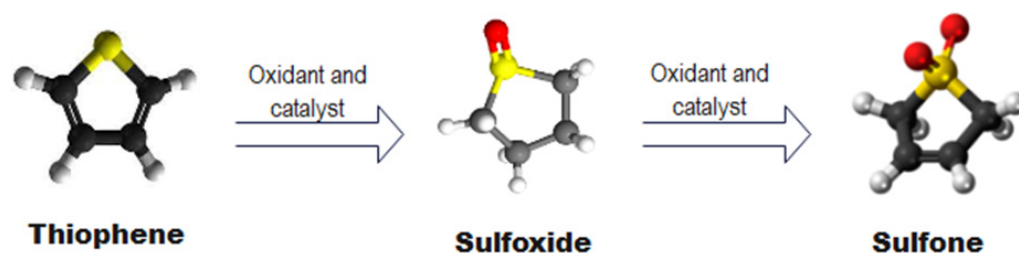


**Figure 1.** The pathway for the ODS process.

Recent studies on the catalytic oxidation desulfurization process have tended to use nano-catalysts. Small metal crystal synthesis is stabilized to a thermally stable support (such as  $\text{Al}_2\text{O}_3$ ,  $\text{SiO}_2$ ,  $\text{TiO}_2$  or  $\text{C}$ ) on a material with a large surface area. The most significant obstacles are preventing the harmful propensity of nanoscale aggregation and synthesizing nanoparticles with regulated nanoscale sizes and shapes [14]. Active carbons (AC) are frequently utilized as adsorbents. They are significant industrial adsorbents that are highly adaptable and frequently used in a variety of applications that are primarily concerned with removing undesirable substances from gases or liquids. Additionally, they are used for gas storage, catalyst supports or catalysts. It was discovered that the variability in the materials' physicochemical catalytic capabilities was caused by the surface function groups attached on the inside carbons [15]. There are further studies being done to improve activated carbon, including loading it with metal oxide, where it can improve the removal of sulfur by adsorption using metal oxides on the basis of AC, which results in electron interactions where sulfur compounds are cycled with metal oxides on the catalyst support [16]. To optimize and enhance the mechanical characteristics of the catalyst, the metals are dispersed over an extensive surface area of a suitable support. It has been found that a number of low-cost metal-based catalysts, including those made of Mn, Co and Mo, are particularly effective at lowering the sulfur content of fuels when subjected to the ODS process [17]. Similar to this, the differing physiochemical properties of Cu- and Ni-based ODS catalysts have attracted a lot of attention [18,19]. However, when they are utilized directly in the catalytic ODS method without a suitable support, these catalysts become difficult to remove from the organic phase [20]. In certain cases, the

deposition of a highly distributed active phase in a support's mesopores can stabilize it. A proper relationship between the catalytically active phase and the support surface can result in a further advantage. This interaction becomes apparent when the catalytic activity reaches its peak at a specific concentration and then increases as a function of the active state concentration at the support surface. The impregnated metals on the activated carbon support, for a catalyst to form a mesoporous structure with a large surface area, are obtained. On the surface of the support, the active species were widely dispersed and the supported catalyst's mesoporous structure remained unaltered. The surface Mo atoms gradually transformed from tetrahedrally coordinated  $\text{Mo}^{6+}$  species toward octahedrally coordinated  $\text{Mo}^{4+}$  as the Mo loading increased. Increasing Mo loading can foster a decrease of Mo species [21].

In this study, four different nano-catalysts [Nickel–Cobalt–Manganese (NCM) (NCM/AC) and Nickel–Cobalt–Manganese with several concentrations of Molybdenum (1 wt%, 2 wt% and 3 wt%) (NCMM) (which are named NCMM\_1/AC, NCMM\_2/AC and NCMM\_3/AC, respectively)] are produced and supported on activated carbon manufactured from apricot shells (agro-wastes). Activated carbon (AC) was chosen as the support due to its substantial specific surface area, low cost, high absorption capacity and ability to be produced directly from biomass resources. Then, the morphological characteristics of such nano-catalysts produced have been investigated using X-ray diffraction (XRD), Fourier transform infrared (FTIR) spectroscopy, BET surface area, pore volume, thermogravimetric analysis (TGA), scanning electron microscopy (SEM) and X-ray fluorescence (XRF). Finally, the performance of sulfur removal from a wide middle distillate (WMD) fuel is evaluated, employing the designed catalysts in a batch oxidative desulfurization process. Air is used as an oxidant within the batch reactor.

## 2. Results and Discussion

### 2.1. Performance Evaluation of the Designed Nano-Catalysts

Several efforts were made to increase the effectiveness of the activated carbon catalyst made from apricot shells by including transition metals such as Co, Ni, Mn, (NCM) and Mo (NCMM) at concentrations of 1%, 2% and 3%. To find the most suitable nonporous catalyst for the ODS process, the impact of loading some of the transition metals on the AC support was assessed. The created nano-catalysts' sulfur was converted using the best ODS catalyst, which was discovered.

#### 2.1.1. Chemical Composition

Utilizing X-ray fluorescence (XRF), the chemical structure of the produced NCM/AC and NCMMAC nano-catalysts is identified. The structural formula of the prepared catalysts is ascertained using XRF, which is also utilized to establish the presence and distribution of the active metal species on the catalyst's substrate. Table 1 provides the chemical composition of the components.

**Table 1.** Chemical composition of elements by XRF.

Component (wt%)	NCM/AC	NCMM_1/AC	NCMM_2/AC	NCMM_3/AC
Carbon (C)	73.1	72.2	71.7	70.9
Oxygen (O)	14.2	18.3	17.4	17.8
Nickel (Ni)	3.89	3.17	3.19	3.18
Cobalt (Co)	1.95	1.49	1.48	1.51
Manganese (Mn)	3.91	3.11	3.06	3.08
Molybdenum (Mo)	0.0	0.96	1.91	2.97

The elements found on the surfaces of NCM/AC, NCMM\_1/AC, NCMM\_2/AC and NCMM\_3/AC have confirmed that the formation of metal nano-catalysts was seen in response to thermal and chemical degradation. All of the samples that were obtained chemically and thermally demonstrated the emergence of different kinds of metal nanoparticles.

Each sample contains metals such as Ni, Mn, Co and Mo, which help with the creation of metal nano-catalysts. Additionally, less than 1% of the total amount of metal oxides is lost.

Such a slight change in the metal oxides material, as validated by the XRF, demonstrates that such metal oxides have uniformly been distributed over the surface of the NCM/AC, NCMM\_1/AC, NCMM\_2/AC and NCMM\_3/AC catalysts without changing the chemical structure of the element or having an impact on the pores produced by AC activation. The weight percent of the metal oxides material shows that the methods used for implementing the required weight percent of such substances have successfully been absorbed [22].

### 2.1.2. SEM Analysis

The scanning electron microscopy (SEM) pictures of each nano-catalyst are shown in Figure 2. SEM analysis was performed on all nano-catalyst metal sample sets, primarily Ni–Co–Mn (NCM/AC) and Ni–Co–Mn–Mo (NCMM\_1/AC, NCMM\_2/AC and NCMM\_3/AC). Based on these pictures, it is observed that there are no noted metal agglomerations on the catalyst generated and that the metals have uniformly been distributed and completely impregnated. This led to a more consistent impregnation being performed [23].

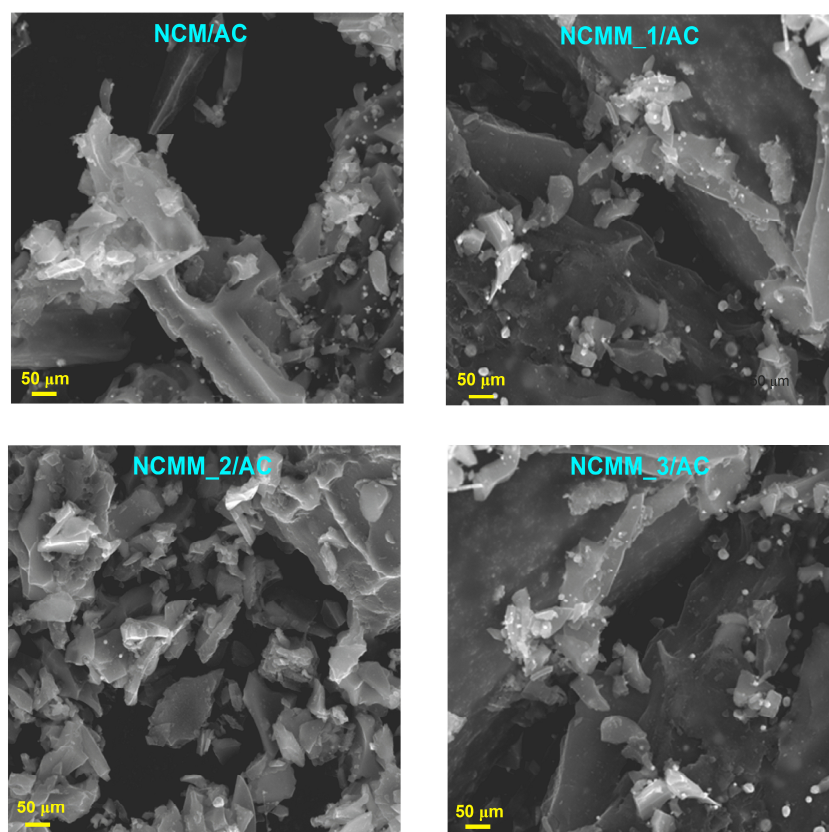


**Figure 2.** SEM images for all the catalysts prepared.

### 2.1.3. Pore Size Distribution Evaluation

The pore size distribution (PSD) for all the catalysts prepared is demonstrated in Figure 3. Regarding this figure, it has been indicated that the mesopores of nano-catalysts are noticed. There are two peaks in the pore size distribution between 20 and 58 nm. Mesopores are dominating at the first maximum, whereas macropores with sizes ranging from 25 to 100 nm are presented at the second maximum. It is thought that the high macroporosity of the activated carbon from apricot shells was caused by the higher cellulose amount found in the precursor (AS) because the source of the precursor had a significant

impact on the structure of the pores of activated carbon generated by the single-step pyrolysis activation procedure used in this research [24].

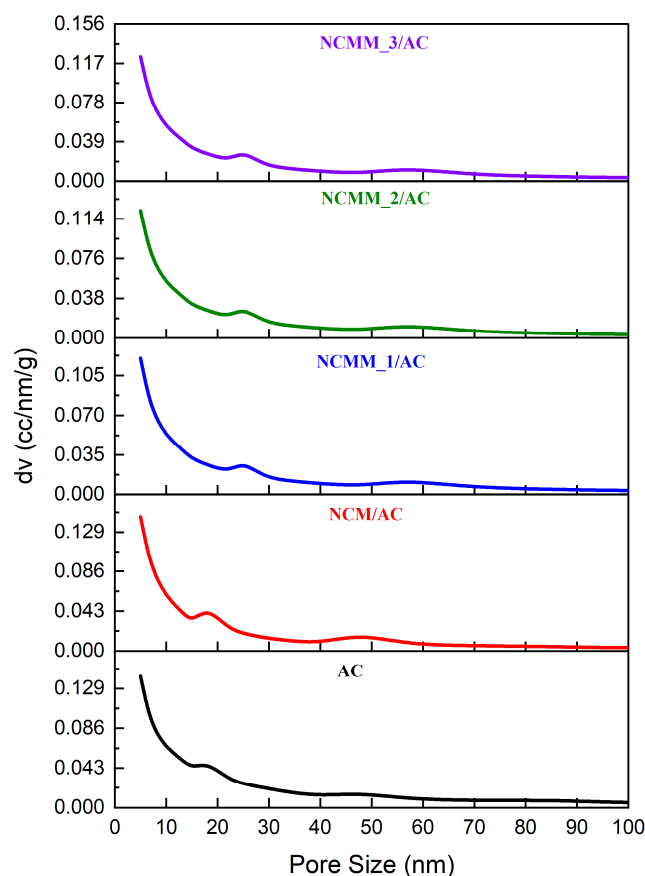


**Figure 3.** PSD analysis for all the catalysts prepared.

#### 2.1.4. Thermographic Analysis (TGA)

The thermal gravimetric analysis (TGA) was used to determine the mass change of the materials during thermal treatment. Figure 4 depicts the TGA thermograms of NCM1/AC, NCM2/AC and NCM3/AC. According to TGA thermograms, NCM2/AC has greater thermal stability than NCM1/AC and NCM3/AC. TGA thermograms revealed two distinct weight reductions. The first weight loss was seen below 300 °C, which can be attributed to water molecules and various oxygen functions being eliminated from the catalyst surface [25–27]. The degradation of carbonaceous materials was caused by the second weight loss at temperatures ranging from 300 to 500 °C. Additionally, no substantial weight loss was found above 500 °C, indicating the catalyst's stability up to 300 °C. These findings show that the synthesized catalyst can be used efficiently for organic transformations up to 300 °C with no significant loss of catalytic activity.

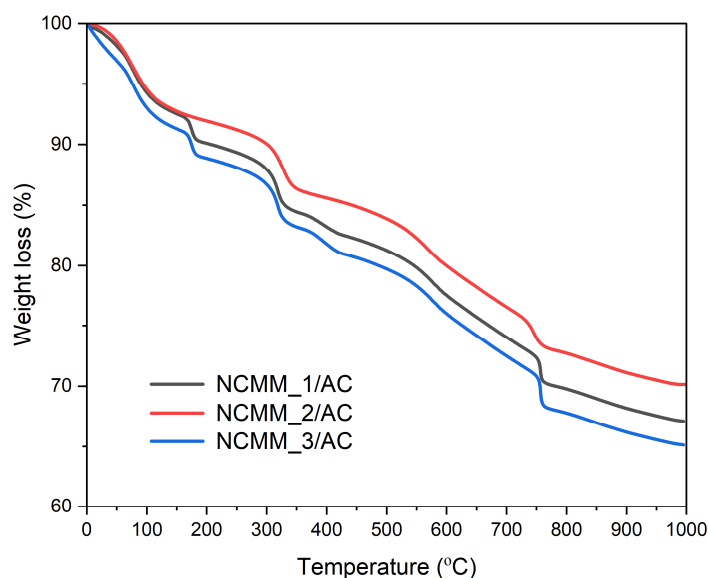


**Figure 4.** TGA analysis for the catalysts prepared.

#### 2.1.5. FTIR Analysis

The Fourier transform infrared (FTIR) functional groups present in the produced activated carbons with the adsorption of metal ions (Ni (II), Co (II), Mn (II) and Mo) were analyzed using FTIR spectroscopy. Figure 5 displays the FTIR spectra of the AC, NCM/AC, NCMM-1/AC, NCMM-2/AC and NCMM-3/AC samples.

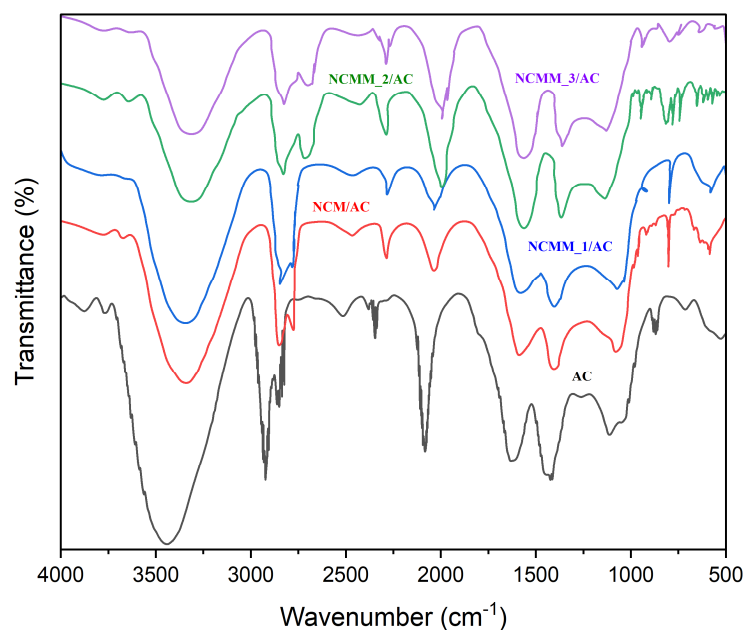


**Figure 5.** FTIR analysis for all the catalysts prepared.

The stretching vibration of the hydroxyl group (O–H) caused by the oscillation of the water molecules is thought to be responsible for a significant band in the AC spectra at  $3440\text{ cm}^{-1}$  [28]. The prominence of the peak at  $2932\text{ cm}^{-1}$  is due to the presence of the aliphatic C–H stretch of the CH, CH<sub>2</sub> and CH<sub>3</sub> groups. The peak at  $2853\text{ cm}^{-1}$  is due to CH<sub>2</sub> symmetric stretching, and the peak at  $2351\text{ cm}^{-1}$  is brought about by the existence of C=C groups. The two peaks ( $2932$ , and  $2853\text{ cm}^{-1}$ ) have been evolved and well separated when AC were loaded with metals, and this was noticed and was more obvious in the NCMM\_2/AC sample than the other samples. This may give the NCMM\_2/AC sample

separated regions of functionalities that will play an important role of giving extra space for reactions.

The peak at  $2084\text{ cm}^{-1}$  is related to the C=N stretching vibrations. The peak at  $1626\text{ cm}^{-1}$  may be connected to the C=O stretching of carboxylic acids. The band at  $1444\text{ cm}^{-1}$  is designated to contain both symmetric and asymmetric C-H bending vibrations [29]. However, metal oxide stretching vibration was linked to peaks between  $640$  and  $430\text{ cm}^{-1}$ . The weak band in the  $900\text{--}1300\text{ cm}^{-1}$  range could be brought on by the sample's C-O group content. The band, which is found at  $836\text{ cm}^{-1}$ , is associated with the stretching vibrations of the C-H out-of-plane band. The FTIR spectra of the tested samples showed all of the functionalities observed in the AC, indicating that metals were physically adsorbed onto the surface of the AC [30–32]. The region between  $500$  and  $1000\text{ cm}^{-1}$  shows that NCMM\_2/AC has the highest peak groups among all the tested samples. Due to its largest functional groups, it is evident from this evidence that NCMM\_2 material will exhibit the highest activity among the other evaluated samples [33].

#### 2.1.6. XRD Analysis

X-ray diffraction (XRD) is the oldest and most popular method for illustrating catalysts. It can be used to pinpoint the catalyst's crystalline condition. The effect of transition metal doping on catalytically enhanced metals (activated carbon) is seen in Figure 6.

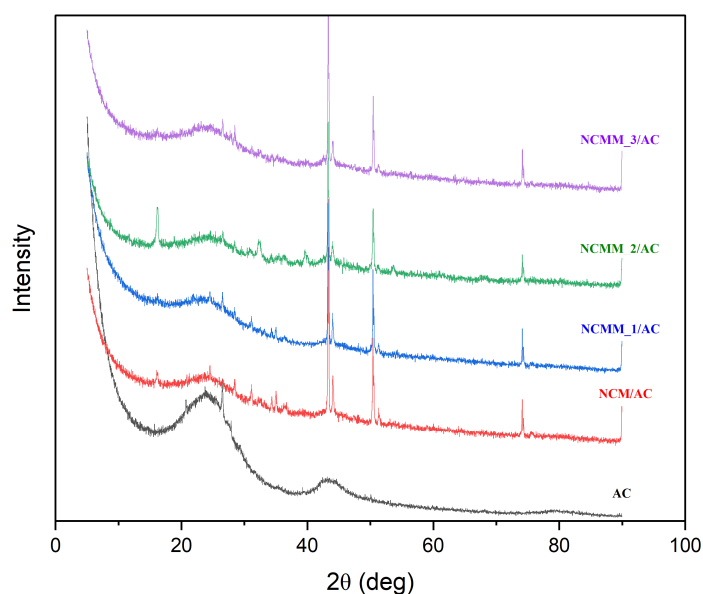


**Figure 6.** XRD analysis for all the catalysts prepared.

The phase angles at the two theta coordinates of  $25.67$  and  $43.28^\circ$  demonstrate the formation of activated carbon. The peaks that appear at  $51.00$  and  $75.34$  degrees are due to NCM and NCMM materials. The displacement of the  $25.67$  peak to the left of the NCM material and even more of the NCMM materials in this figure may be attributable to the enhancement of the structural stability of the transition metal-impregnated activated carbon, which is the most significant and obvious evidence [34]. NCMM is therefore anticipated to exhibit the highest level of activity. These results are consistent with those from FTIR and TGA results.

#### 2.1.7. Surface Area and Pore Volume

The surface area and pore volume of the catalysts should be determined since they have an impact on the catalytic activity and mass transfer of reactants and products [29]. The surface area (BET), pore volume and average pore diameter of the activated carbon and nano-catalyst NCM/AC, NCMM\_1/AC, NCMM\_2/AC and NCMM\_3/AC adsorbents

were determined using the nitrogen adsorption–desorption method. Figure 7 presents these outcomes.

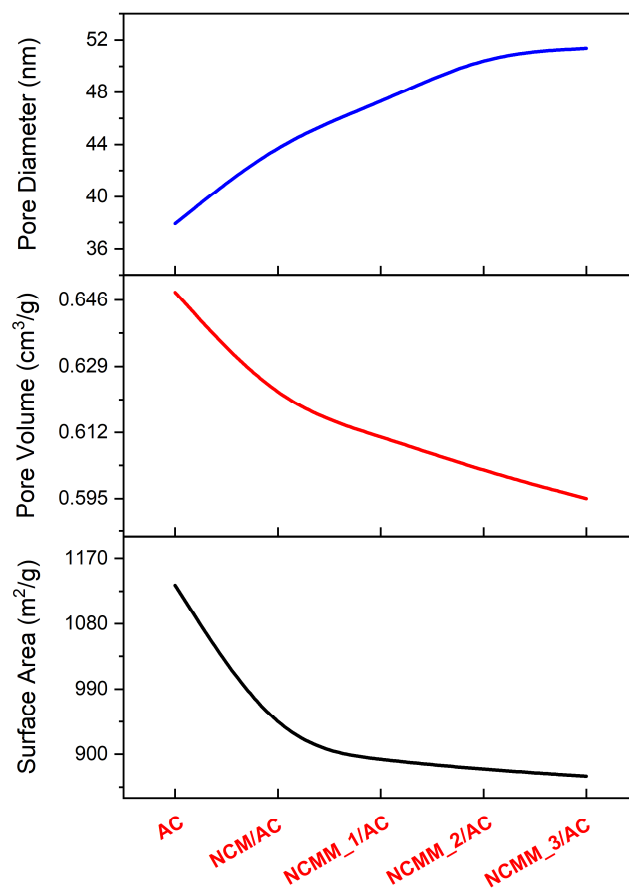


**Figure 7.** Surface area, pore volume and pore diameter for all the catalysts prepared.

These findings show that the surface area of the created AC was 1133.347 m<sup>2</sup>/g, the pore diameter was 37.92 nm and the total volume of the pores was 0.648 cm<sup>3</sup>/g. Such recent investigations, which include the high surface area and pore volume of AC from an unpublished source (AS), are thought to be original and imaginative and will have a positive impact on the catalysts developed.

After the impregnation process with loading of active metals (Ni, Co, Mn) for NCM and (Ni, Co, Mn and Mo (1%, 2% and 3%)) for NCMM\_1/AC, NCMM\_2/AC and NCMM\_3/AC, the surface area and pore volume were slightly reduced, with opposite phenomenon related to the average pore diameter. This behavior in the mesopores' surface area, pore volume and diameter is explained by NCM oxides filling part of the AC's vacant sites. As a result, there is a possibility of decreasing the surface area and other properties for the adsorption process.

This slight drop shows that most of the catalyst's external surface was impregnated with the NCMM material and that there was no migration of the loaded material particles into the interior pores. Additionally, the surface area available for adsorption would be hardly affected by such reduction. This attitude of the catalytic material typically decreases as the amount of the active component increases until the monolayer coverage of the impregnated component is achieved [35].

In comparison to those described in the literature, the new results obtained here regarding surface area and pore volume are still very high, and pore diameter is still small (mesoporous nanomaterial). This finding has rendered clear evidence, based on the results established during the preparation process, that the active component supplied to the support may be applied to the ODS responses with great certainty. As a result, the

produced catalysts' large surface area and pore volume and mesoporous material might offer several chemically active places for the associated processes.

## 2.2. Evaluation of the Catalysts Using Batch Reactor

The activity of the prepared catalysts, NCM, NCMM\_1/AC, NCMM\_2/AC and NCMM\_3/AC, is being investigated here with respect to the oxidative desulfurization technique of the Iraqi wide distillate fraction ranging from IBP to 345 °C.

Air is used as an oxidant in a batch reactor under conditions that include an air flow rate of 120 L/h, reaction temperature of 363 K and batch reaction time of 1 h for all catalysts. It is common knowledge that sulfur compounds have a slight polarity advantage over hydrocarbons with similar structures. The sulfur oxidizers, sulphones and sulfoxide, are substantially more polar than sulfur dioxide. More crucially, compared to most hydrocarbons, the conversion of sulphones from sulfides is frequently much easier and quicker [36]. Experimental results on catalyst activity in the oxidation process for all the catalysts prepared are shown in Figure 8.

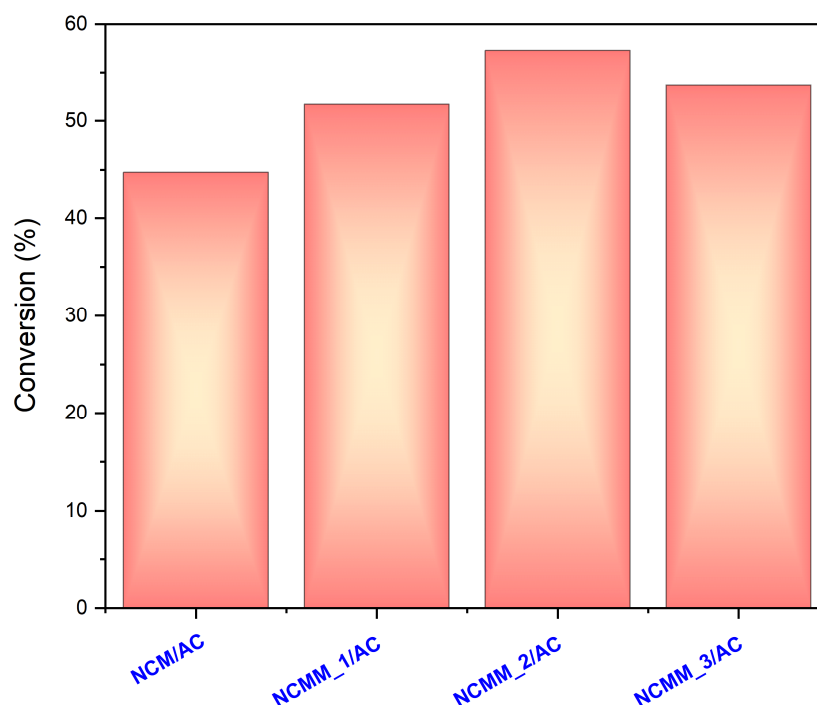


**Figure 8.** Sulfur conversion for all the catalysts prepared.

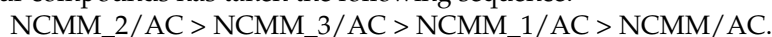
Depending on the outcomes from this figure, the catalysts developed here can be employed for sulfur removal from oil fractions.

Additionally, an enhancement in the catalyst's active sites is observed when increasing the concentration of the Molybdenum (Mo) component (under the same process conditions) up to 2 wt%, leading to an improvement in the conversion of sulfur compounds, then it decreases at 3 wt% of Mo, and these catalysts behave identically under process circumstances.

The NCMM\_2/AC and NCMM\_3/AC catalysts act more actively than the NCM/AC and NCMM\_1/AC catalysts. Because NCMM/AC at 2 and 3 wt% of Mo has the largest active compound loading of all the catalysts and its activity is higher than that of the NCM/AC and NCMM\_1/AC catalysts, adding the Mo to enhance the activity of the NCM/AC catalysts is stated to create an improvement by increasing the reactivity of sulfur removal. The biggest sulfur removal has been obtained with NCMM\_2/AC, owing to its cations close to the catalyst surface, and based on the conversion results, NCMM\_3/AC has less of such cations near the catalyst surface compared to NCMM\_2/AC. The catalysts' activities, which are related to their large surface areas, are attributed to this phenomenon.

More active sites are made accessible for the adsorption of refractory sulfur compounds as Mo is added by 1 wt% and 2 wt%, and the opposite behavior begins at 3 wt%. The surface support that covers it also fills the pores. The efficiency of the desulfurization process is significantly influenced by the properties of the metal loaded beside the support material represented by AC [37–39].

Chemical interactions between the metals deposited on the catalyst surface and physical variables resulting from the adsorption behavior are the main factors controlling the complex sulfur removal process. Thus, the acidic site of the AC support helps to remove substituted sulfur compounds by enhancing the activity of the active metals via adding the Mo up to 2 wt%. Finally, the order of the catalysts prepared regarding the removal of sulfur compounds has taken the following sequence:



### 3. Experiment

#### 3.1. Materials and Chemicals

The wide middle distillate (WMD) cut supplied by the North Refineries Company (Baiji refinery), located in Baiji, Iraq, is used as a main oil feedstock for ODS reactions. The main properties of the chemical components utilized to create nano-catalysts as well as the WMD are listed in Tables 2 and 3, respectively.

**Table 2.** A list of the materials and chemicals used.

Chemicals	Formula	Purity%	Company
Nickel acetate tetra hydrate	$(\text{CH}_3\text{COOH})_2\text{Ni}\cdot 4\text{H}_2\text{O}$	99	Thomas Baker, London, UK
Manganese (III) acetate hydrate	$(\text{CH}_3\text{COO})_2\text{Mn}\cdot 2\text{H}_2\text{O}$	99	Thomas Baker, London, UK
Cobalt Chloride hexa hydrate	$\text{CoCl}_2\cdot 6\text{H}_2\text{O}$	99	Thomas Baker, London, UK
Ammonium Molybdate tetra hydrate	$(\text{NH}_4)_6\text{Mo}_7\text{O}_{24}\cdot 4\text{H}_2\text{O}$	99	Thomas Baker, London, UK
Deionized water	$\text{H}_2\text{O}$	pH = 7.0 TDS = 0.0	Analytical chemicals lab—Chemical Engineering Department/Tikrit, Tikrit, Iraq
Acetonitrile	$\text{C}_2\text{H}_3\text{N}$	99.9	Concord Technology, Ramtekdi, India

**Table 3.** Characteristics of wide middle distillate fuel.

Factors	Specifications
Sp.gr @ 15.6 C	0.7708
Sulfur content	4826 ppm
Initial boiling point	29 °C
End boiling point	345 °C
API	52.08

#### 3.2. Nano-Catalysts Preparation

##### 3.2.1. Activated Carbon Preparation

Activated carbon (AC) was prepared from the local apricot shells (AS) by washing, drying, crushing, grinding and sizing to 40 mesh. Then, chemical treatment was carried out by involving phosphoric acid treatment with AS, wherein AS was impregnated with  $\text{H}_3\text{PO}_4$  and dried overnight in an oven for acid evaporation. The product was washed with hot deionized water, pH was measured, and the product was carbonized using a tubular furnace at 500 °C for 2 h. The second treating was conducted using  $\text{HNO}_3$  at a 50% concentration that was treated with AC and immersed for two hours at 70 °C. A pH meter was used to neutralize the sample after washing it with deionized water, and the purified AC was dried overnight.

### 3.2.2. Metals Loading and Chemical Activation

To prepare 100 g of each nano-catalyst by using the incipient wetness impregnation method (IWI), 10 wt% NCM mixture was firstly dissolved in deionized water, mixed with AC support and sonicated for 80 min. The mixture was heated at 60 °C, dried and calcinated in a tubular furnace under N<sub>2</sub> gas for 2 h. Whereas for different NCMM catalysts, a mixture including 10 wt% of metals (Nickel–Cobalt–Manganese and Molybdenum) was separately weighted in a beaker and dissolved in deionized water to create the nano-catalysts containing 1 wt%, 2 wt% and 3 wt% of Mo supported on activated carbon. The salts used were Nickel acetate tetrahydrate, Cobalt Chloride hexahydrate, Manganese (III) acetate hydrate and Ammonium Molybdate tetrahydrate. Table 4 shows the amount of salts and deionized water that was used in preparing nano-catalysts. The solution was then stirred with a magnetic stirrer for 30 min at room temperature to produce a saturated solution. In a beaker, 90 g of AC nanoparticles was weighed, added to the metals solution and mixed for 15 min at room temperature using a magnetic stirrer. The liquid was thoroughly blended for eighty minutes and left overnight in a sonicator or an ultrasonic homogenizer mixer. Then, solutions of impregnated AC were loaded in a crucible and heated at 120 °C overnight to dry the mixture. After that, the catalysts were calcinated in a tubular furnace for two hours at 850 °C with 99.99% pure N<sub>2</sub> gas. The steps for preparing nano-catalysts are summarized in Figure 9.

**Table 4.** The quantity of salts and deionized water used for catalysts preparation.

Sample	Metal	Weight (%)	Salt (g)	Total Deionized Water (mL)
NCM	Ni	4.0	16.96	1748.91
	Co	2.0	8.07	
	Mn	4.0	19.52	
NCMM_1/AC	Ni	3.6	15.30	1678.63
	Co	1.8	7.30	
	Mn	3.6	17.60	
	Mo	1.0	1.20	
NCMM_2/AC	Ni	3.2	13.60	1607.85
	Co	1.6	6.50	
	Mn	3.2	15.60	
	Mo	2.0	2.40	
NCMM_3/AC	Ni	2.8	11.88	1537.12
	Co	1.4	5.65	
	Mn	2.8	13.67	
	Mo	3.0	3.60	

The X-ray fluorescence (XRF) test was measured using X-ray fluorescence spectroscopy, ametek type, Samson, Turkey. The scanning electron microscopy (SEM) was studied using the Jeol JSM-7001F process, Samson, Turkey. The pore size distribution (PSD) was determined by the Dubinin–Astakhov (DA) method. Thermal gravimetric analysis (TGA) has been carried out using the TGA Q600 technique, Samson, Turkey. The Fourier transform infrared (FTIR) was evaluated by the FTIR spectrophotometer, SHIMADZU device, Samson, Turkey. The X-ray diffraction (XRD) was performed using a diffractometer (PANalytical; X'Pert PRO MPD) method, Advanced Technologies Research and Applications Center/ Samson, Turkey. The surface area was measured using the Brunauer–Emmett–Teller (BET) method (Quantachrome Instrument's), Samson, Turkey, while the pore volume was determined via the Dubinin–Radushkevich (D–R) technique.

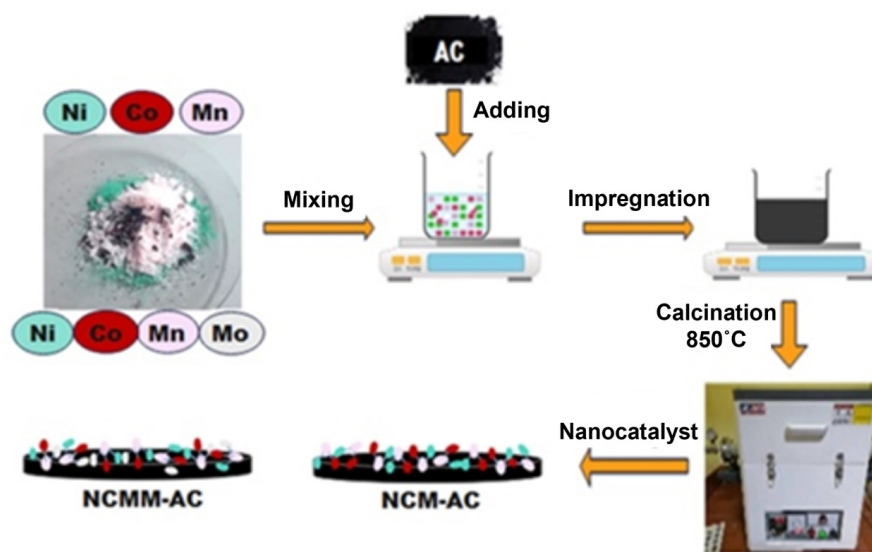


**Figure 9.** The steps for all nano-catalysts prepared.

### 3.3. Evaluation of the Catalysts Performances

#### 3.3.1. Batch Reactor

In a batch reactor, the oxidation reaction is carried out. To evaluate and carrying out tests on the sulfur removal of the designed catalysts, the reaction is conducted in a 500 mL flask with three necks and a circular bottom. To allow air to escape, the middle neck is connected to a vertical condenser that condenses the vapor from the WMD fuel. The second neck is connected to the compressor to provide the air inlet required (the oxidant). The air is charged to the bottom of the flask by the glass tube. The third neck is used to measure the temperature in the flask by entering a thermometer into the solution inside the flask and removing the sample reaction when the time is approaching. The batch reactor is heated and mixed through the use of a heating mantle stirrer.

#### 3.3.2. Conditions of Process

The batch reactor runs with a magnetic stirrer, a heating mantle, nano-catalyst NCM/AC, NCMM\_1/AC, NCMM\_2/AC and NCMM\_3/AC, a flow rate of air of 120 L/h, constant pressure at 1 atm, temperature at 363 K and the reaction time of one hour.

#### 3.3.3. Sulfur Compound Oxidation (ODS Reaction)

The oil feedstock is a wide middle distillate (WMD) fuel, which includes 4826 ppm sulfur content. The equipment is set up to carry out all of the experiments, and each run includes the following steps. The round-bottom flask is charged with 300 mL of feedstock. The heating mantle stirrer, air tube and condenser are all attached to the flask. It is established that cooling water is moving through a condenser to stop any feed from evaporating. To measure the temperature of the reaction, a thermometer is inserted. While the needed temperature is reached, 3 g of each nano-catalyst is separately uploaded to the reactor with the compressor, and the time is recorded. The heating mantle stirrer is stopped, and the product undergoes an extraction procedure. At the finish of each run, the reactor is cleaned and dried, and the next run is prepared. The batch reactor's process is seen in Figure 10.

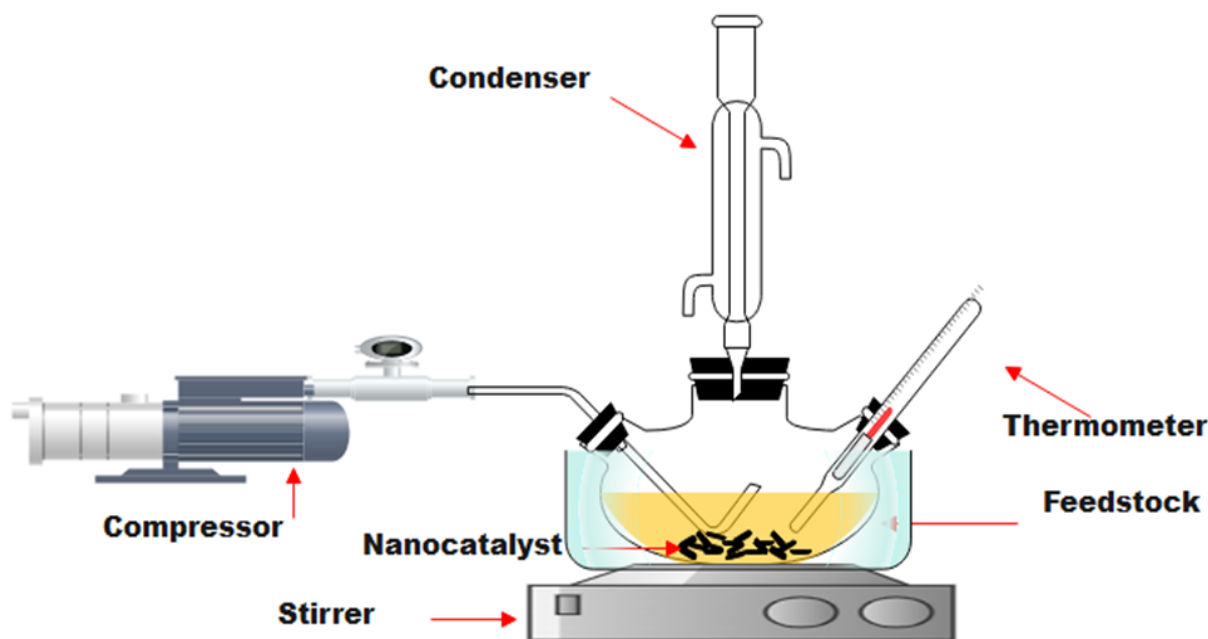


Figure 10. The ODS experimental equipment.

### 3.3.4. Extraction

The resultant reaction mixture was then allowed to cool to room temperature before the acetonitrile solvent ( $C_2H_3N$ ) was added to a 1:1 volume ratio to extract the oxidation compounds. The immiscible mixture was created by using a 250 mL separating funnel for 2 h. The bottom of the funnel represents the clear liquid middle distillate fuel (WMD oxidized), while the top phase of the liquid in the funnel is the sulfone compounds extracted by the extraction process, which is illustrated in Figure 11.

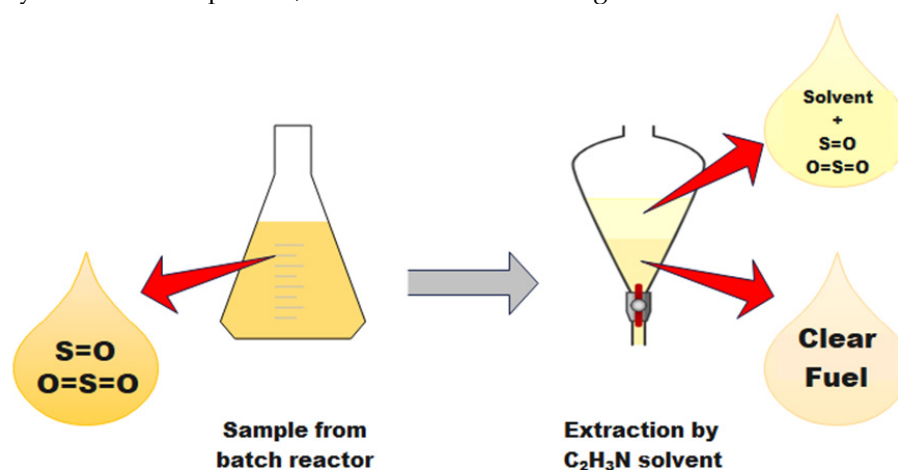


Figure 11. An extraction process diagram.

### 3.3.5. Sample Examination

All the samples of feedstock and products were examined for sulfur levels in the Petroleum Laboratory at Tikrit University-Iraq, in accordance with ASTM D7039. The following formula has been utilized for calculating the conversion of sulfur compounds during the oxidation reactions:

$$ODS\% = \frac{S_f - S_p}{S_f} \times 100\%$$

where the sulfur concentrations in feed and product are  $S_f$  and  $S_p$ , respectively.

All analytical methods used to determine the characteristics of the prepared catalysts, oil feedstock and final products were precise, quick and repeatable. Each sample has been tested and evaluated based on two iterations of the product analysis at each catalyst. In order to guarantee the correctness of the results, average results from each test have been considered with a maximum variance of 1% over all runs.

#### 4. Conclusions

This work describes the production of unique activated carbon (AC) made from agro-waste (which is apricot shells (AS)), which is then loaded with a combination of metals (Mn, Co and Ni (NCM/AC), as well as Mn, Co, Ni and Mo (NCMM\_1/AC, NCMM\_2/AC and NCMM\_3/AC) utilizing the wetness impregnated technique. From an environmental standpoint, producing AC from AS is safe, affordable and beneficial to the environment. It has been addressed that great outcomes for a nanomaterial with a high surface area and pore volume with mesopore diameter and outstanding other features may be attained based on the study's new approach for producing the AC from the least expensive basic ingredients (AS). This approach is effective for creating nano-catalysts because of the high pore volume and surface area and significant dispersion of the active metal. The active chemical is mostly accountable for the catalyst's efficiency.

By analyzing the textural properties of the catalysts prepared using FTIR, XRD, XRF, TGA, SEM and surface area, as well as pore volume and diameter, it was determined that these catalysts had excellent metal loading. The outcomes also showed that the NCMM\_2/AC nano-catalyst eliminates more sulfur than the NCM/AC, NCMM\_1/AC and NCMM\_3/AC nano-catalysts. The new home-made nano-catalysts were capable of being utilized in oxidative desulfurization reactions with high confidence considering the characteristics of the process conversion established here, and the catalyst NCMM\_2/AC was addressed as being the most significant catalyst. The use of Molybdenum (Mo) material can improve the thermal stability and activity of the NCM/AC by increasing the concentration up to 2 wt%, resulting in high sulfur removal by the ODS reaction of the wide middle distillate fuel, whereas the opposite behavior was noted at higher than this percent of Mo.

**Author Contributions:** Conceptualization, S.A.H. and R.B.A.; methodology, I.M.M. and K.I.H.; software, A.T.J. and S.A.H.; validation, A.T.J. and K.I.H.; formal analysis, A.T.J. and I.M.M.; investigation, S.A.H. and A.T.J.; resources, K.I.H.; data curation, S.A.H. and R.B.A.; writing—original draft preparation, S.A.H. and K.I.H.; writing—review and editing, I.M.M. and A.T.J.; visualization, R.B.A. and A.T.J.; supervision, I.M.M. and A.T.J.; project administration, I.M.M. All authors have read and agreed to the published version of the manuscript.

**Funding:** This research received no external funding.

**Data Availability Statement:** All data used in the study appear in the submitted article.

**Conflicts of Interest:** The authors declare no conflict of interest.

#### References

1. Srivastava, V.C. An evaluation of desulfurization technologies for sulfur removal from liquid fuels. *RSC Adv.* **2012**, *2*, 759–783. [[CrossRef](#)]
2. Khan, N.A.; Hasan, Z.; Jhung, S.H. Adsorptive removal of hazardous materials using metal–organic frameworks (MOFs): A review. *J. Hazard. Mater.* **2013**, *244–245*, 444–456. [[CrossRef](#)]
3. Ma, X.; Sakanishi, K.; Isoda, T.; Mochida, I. Hydrodesulfurization reactivities of narrow-cut fractions in a gas oil. *Ind. Eng. Chem. Res.* **2002**, *34*, 748–754. [[CrossRef](#)]
4. Ma, X.; Sakanishi, K.; Mochida, I. Hydrodesulfurization reactivities of various sulfur compounds in diesel fuel. *Ind. Eng. Chem. Res.* **1994**, *33*, 218–222. [[CrossRef](#)]
5. Ancheyta, J. *Handbook of Deactivation of Heavy Oil Hydroprocessing Catalysts: Fundamentals and Modeling*, 1st ed.; John Wiley & Sons, Inc.: Hoboken, NJ, USA, 2016.
6. Bakar, W.A.W.A.; Ali, R.; Kadir, A.A.A.; Mokhtar, W.N.A.W. The Role of Molybdenum Oxide Based Catalysts on Oxidative Desulfurization of Diesel Fuel. *Mod. Chem. Appl.* **2015**, *3*, 150.
7. Rang, H.; Kann, J.; Oja, V. Advances in Desulfurization Research of Liquid Fuel. *Oil Shale* **2006**, *23*, 164–176. [[CrossRef](#)]

8. Zannikos, F.; Lois, E.; Stournas, S. Desulfurization of petroleum fractions by oxidation and solvent extraction. *Fuel Process. Technol.* **1995**, *42*, 35–45. [[CrossRef](#)]
9. Otsuki, S.; Nonaka, T.; Takashima, N.; Qian, W.; Ishihara, A.; Imai, T.; Kabe, T. Oxidative Desulfurization of Light Gas Oil and Vacuum Gas Oil by Oxidation and Solvent Extraction. *Energy Fuels* **2000**, *14*, 1232–1239. [[CrossRef](#)]
10. Campos-Martin, J.M.; Capel-Sanchez, M.C.; Perez-Presas, P.; Fierro, J.L.G. Oxidative processes of desulfurization of liquid fuels. *J. Chem. Technol. Biotechnol.* **2010**, *85*, 879–890. [[CrossRef](#)]
11. Houda, S.; Lancelot, C.; Blanchar, P.; Poinel, L.; Lamonier, C. Oxidative Desulfurization of Heavy Oils with High Sulfur Content: A Review. *Catalysts* **2018**, *8*, 344. [[CrossRef](#)]
12. Karas, L.J.; Han, Y.Z.; Leyshon, D.W. Organosulfur Oxidation Process. U.S. Patent 2,004,178,122, 16 September 2004.
13. Kocal, J.A.; Branvold, T.A. Removal of Sulfur-Containing Compounds from Liquid Hydrocarbon Streams. U.S. Patent 6,368,495, 9 April 2002.
14. Jarullah, A.T.; Ahmed, A.M.; Hussein, H.M.; Ahmed, A.N.; Mohammed, H.J. Evaluation of synthesized Pt/HY-H-Mordenite composite catalyst for Isomerization of Light Naphtha. *Tikrit J. Eng. Sci.* **2023**, *30*, 46–59. [[CrossRef](#)]
15. Al-Ghouti, M.A.; Al-Degs, Y.S.; Khalili, F.I. Minimisation of organosulphur compounds by activated carbon from Diesel fuel: Mechanistic study. *Chem. Eng. J.* **2010**, *162*, 669–676. [[CrossRef](#)]
16. Ahmedzeki, N.S.; Ali, S.M.; Al-Karkhi, S.R. Synthesis and Characterization of Tri-Composite Activated Carbon. *Iraqi J. Chem. Pet. Eng.* **2017**, *18*, 49–58. [[CrossRef](#)]
17. Alheety, M.A.; Al-Jibori, S.A.; Karadağ, A.; Akbaş, H.; Ahmed, M.H. A novel synthesis of MnO<sub>2</sub>, nanoflowers as an efficient heterogeneous catalyst for oxidative desulfurization of thiophenes. *Nano-Struct. Nano-Objects* **2019**, *20*, 100392. [[CrossRef](#)]
18. Sarda, K.K.; Bhandari, A.; Pant, K.K.; Jain, S. Deep desulfurization of diesel fuel by selective adsorption over Ni/Al<sub>2</sub>O<sub>3</sub> and Ni/ZSM-5 extrudates. *Fuel* **2012**, *93*, 86–91. [[CrossRef](#)]
19. Wei, S.; He, H.; Cheng, Y.; Yang, C.; Zeng, G.; Kang, L.; Qian, H.; Zhu, C. Preparation, characterization, and catalytic performances of cobalt catalysts supported on KIT-6 silicas in oxidative desulfurization of dibenzothiophene. *Fuel* **2017**, *200*, 11–21. [[CrossRef](#)]
20. Sikarwar, P.; Arun Kumar, U.K.; Gosu, V.; Subbaramaiah, V. Catalytic oxidative desulfurization of DBT using green catalyst (Mo/MCM-41) derived from coal fly ash. *J. Environ. Chem. Eng.* **2018**, *6*, 1736–1744. [[CrossRef](#)]
21. Lv, M.; Xie, W.; Sun, S.; Wu, G.M.; Zheng, L.; Chu, S.; Gao, C.; Bao, J. Activated-carbon-supported K-Co-Mo catalyst for synthesis of higher alcohols from syngas. *Catal. Sci. Technol.* **2015**, *5*, 2925–2934. [[CrossRef](#)]
22. Jarullah, A.T.; Ahmed, A.N.; Ban, A.A.; Ahmed, A.M. Design of New Composites Nano-Catalysts for Naphtha Reforming Process: Experiments and Process Modeling. *Tikrit J. Eng. Sci.* **2023**, *30*, 94–103. [[CrossRef](#)]
23. De Mello, S.; Sobrinho, E.V.; da Silva, T.; Pergher, S.B.C. V or Mn zeolite catalysts for the oxidative desulfurization of diesel fractions using dibenzothiophene as a probe molecule: Preliminary study. *Mol. Catal.* **2020**, *482*, 100495. [[CrossRef](#)]
24. Petrova, B.; Budinova, T.; Tsyntarski, B.; Kochkodan, V.; Shkavro, Z.; Petrov, N. Removal of aromatic hydrocarbons from water by activated carbon from apricot stones. *Chem. Eng. J.* **2010**, *165*, 258–264. [[CrossRef](#)]
25. Pourkhalil, M.; Moghaddam, A.; Rashidi, A.; Towfighi, J.; Mortazavi, Y. Preparation of highly active manganese oxides supported on functionalized MWNTs for low temperature NO<sub>x</sub> reduction with NH<sub>3</sub>. *Appl. Surf. Sci.* **2013**, *279*, 250–259. [[CrossRef](#)]
26. Haw, K.; Abu Bakar, W.; Ali, R.; Chong, J.; Kadir, A. Catalytic oxidative desulfurization of diesel utilizing hydrogen peroxide and functionalized-activated carbon in a biphasic diesel–acetonitrile system. *Fuel Process. Technol.* **2010**, *91*, 1105–1112. [[CrossRef](#)]
27. Zhao, C.; Jiang, E.; Chen, A. Volatile production from pyrolysis of cellulose, hemicellulose and lignin. *J. Energy Inst.* **2017**, *90*, 902–913. [[CrossRef](#)]
28. Contescu, I.; Adhikari, P.; Gallego, C.; Evans, D.; Biss, E. Activated Carbons Derived from High-Temperature Pyrolysis of Lignocellulosic Biomass. *C J. Carbon Res.* **2018**, *4*, 51. [[CrossRef](#)]
29. Tchalala, R.; El-Demellawi, K.; Abou-Hamad, E. Hybrid electrolytes based on ionic liquids and amorphous porous silicon nanoparticles: Organization and electrochemical properties. *Appl. Mater.* **2017**, *9*, 10–20. [[CrossRef](#)]
30. Saleh, A. The influence of treatment temperature on the acidity of MWCNT oxidized by HNO<sub>3</sub> or a mixture of HNO<sub>3</sub>/H<sub>2</sub>SO<sub>4</sub>. *Appl. Surf. Sci.* **2011**, *257*, 7746–7751. [[CrossRef](#)]
31. Bazrafshan, A.; Hajati, S.; Ghaedi, M. Synthesis of regenerable Zn(OH)<sub>2</sub> nanoparticleloaded activated carbon for the ultrasound-assisted removal of malachite green: Optimization, isotherm and kinetics. *RSC Adv.* **2015**, *5*, 79119–79128. [[CrossRef](#)]
32. Abdul-Kadhim, W.; Deraman, M.; Abdullah, S.; Tajuddin, S.; Yusoff, M.; Taufiq-Yap, Y.; Rahim, M. Efficient and reusable iron-zinc oxide catalyst for oxidative desulfurization of model fuel. *J. Environ. Chem. Eng.* **2017**, *5*, 1645–1656. [[CrossRef](#)]
33. Saleh, A. Isotherm, kinetic, and thermodynamic studies on Hg (II) adsorption from aqueous solution by silica-multiwall carbon nanotubes. *Environ. Sci. Pollut. Res.* **2015**, *22*, 16721–16731. [[CrossRef](#)]
34. Hamin, J.M.; Aysar, T.J.; Ban, A.A.; Hala, M.H. Preparation of synthetic composite nano-catalyst for oxidative desulfurization of kerosene. *Energy Sources Part A Recovery Util. Environ. Eff.* **2023**, *45*, 1672–1685.
35. Jarullah, A.T.; Aldulaimi, S.K.; Al-Tabbakh, B.A.; Mujtaba, I.M. A new synthetic composite nano-catalyst achieving an environmentally friendly fuel by batch oxidative desulfurization. *Chem. Eng. Res. Des.* **2020**, *160*, 405–416. [[CrossRef](#)]
36. Ying, C.; Huixiang, W.; Ruimin, D.; Liancheng, W.; Zhong, L.; Baoliang, L. Highly efficient oxidative desulfurization of dibenzothiophene using Ni modified MoO<sub>3</sub> catalyst. *Appl. Catal. A Gen.* **2020**, *589*, 117308.
37. Iovik, Y.A.; Krivtsov, E.B. Thermal Transformations of Sulfur-Containing Components of Oxidized Vacuum Gas Oil. *Pet. Chem.* **2020**, *60*, 341–347. [[CrossRef](#)]

38. Akopyan, A.V.; Plotnikov, D.A.; Polikarpova, P.D.; Kedalo, A.A.; Egazar'yants, S.V.; Anisimov, A.V.; Karakhanov, E.A. Deep Purification of Vacuum Gas Oil by the Method of Oxidative Desulfurization. *Pet. Chem.* **2019**, *59*, 975–978. [[CrossRef](#)]
39. WanXin, Y.; Guoqing, G.; Zhihong, M.; Yinghao, Y. Deep oxidative desulfurization of model fuels catalysed by immobilized ionic liquid on MIL100(Fe). *RSC Adv.* **2019**, *9*, 21804.

**Disclaimer/Publisher's Note:** The statements, opinions and data contained in all publications are solely those of the individual author(s) and contributor(s) and not of MDPI and/or the editor(s). MDPI and/or the editor(s) disclaim responsibility for any injury to people or property resulting from any ideas, methods, instructions or products referred to in the content.